OPTICS, LASERS, AND QUANTUM ELECTRONICS

A.A. GENERAL, YU.O. SHPENIK

Institute of Electron Physics, Nat. Acad. of Sci. of Ukraine
(21, Universytets'ka Str., Uzhgorod 88017, Ukraine; e-mail: heneral-andrij@rambler.ru)

PACS 52.80.Tn; 52.20.-j

MODELING OF GAS DISCHARGE IN WATER VAPOR

The results of our study of a gas-discharge plasma in water vapor are reported. The generation rate of excited OH^* $(A^2\Sigma^+)$ radicals in the water vapor discharge turns out significantly higher than the formation rate of emitting states of hydrogen and oxygen atoms. According to our estimations, the optimum value of E/N-ratio between the electric field strength E and the concentration of gas particles N for the excitation of radical OH^* bands equals $(300 \div 400) \times \times 10^{-21}$ V·m^2.

K e y w o r d s: gas discharge, radical, rate constant

1. Introduction

Not only lasers, but also sources of spontaneous ultraviolet (UV) radiation find more and more wide applications in ecology, microelectronics, medicine, and other domains of human activity [1]. The most powerful and efficient sources of noncoherent radiation in the UV spectral range are mercury lamps [2]. At the same time, an increasing interest is drawn to UV emitters based on water vapor, because of the environmentally safe and inexpensive working medium that is used in them. Therefore, the research of the parameters of such radiation sources is challenging [3–6]. Their main advantage in comparison with mercury-containing lamps is the absence of mercury in the working medium so that there is no adverse effect to the environment in the course of their subsequent recycling.

Water vapor can be excited with the use of electric discharges of various types and at various pressures in gas mixtures. As a rule, a dc glow discharge and low-pressure high- and ultrahigh-frequency discharges are used. In order that water vapor emit UV radiation with a large pulse power, the application of a barrier discharge is promising [7, 8]. In this case, the highest average powers of UV radiation are generated. When an emitter with open electrodes operates, the

by-products of the water molecule destruction interact with metal electrodes. Under gas-static working conditions, this leads to a reduction of the service life of such an UV emitter. Therefore, it is necessary that the working medium in gas-discharge lamps with open electrodes should be permanently restored, e.g., by pumping water vapor along the gas-discharge tube. However, under gas-static conditions, the application of the barrier discharge becomes possible.

Typical parameters of a barrier-discharge plasma are as follows: the degree of gas ionization is 10^{-1} to 1, electric field strength is up to 100 kV/cm, energy of electrons is up to 20 eV, electron concentration is 10^{12}–10^{15} cm^{-3}, typical gas pressures are up to 10^5 Pa and higher, and typical values of reduced (per one particle) electric field are up to 600 Td, where 1 Td $= 10^{-21}$ V·m^2.

In this work, we carried out a theoretical study of characteristics and electron parameters of the barrier discharge in water vapor (see work [8]) in order to improve the power characteristics of a gas-discharge plasma.

2. Theory and Calculation Procedure

To calculate the electron energy distribution functions (EEDFs), the average energy and the transport coefficients of electrons, the rate constants for elastic and inelastic interactions of electrons with atoms,

and the electron energy losses, we used the software program Bolsig+, which was described in work [9] in detail. The program Bolsig+ can be used for the calculation of the transport coefficients of electrons and rate constants, which are necessary for the modeling of gas discharges in the framework of hydrodynamic models [9].

To calculate the EEDF in the water vapor discharge, we have preliminarily prepared a file with the values of cross-sections of the elastic and inelastic interaction processes with water molecules. The following processes were taken into account:

1) momentum transfer at collisions of electrons with water molecules,
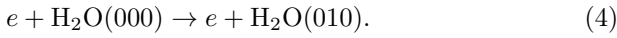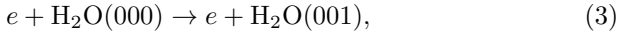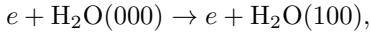
$$e + \mathrm{H_2O} \rightarrow e + \mathrm{H_2O}. \tag{1}$$

2) rotational excitations of water molecules,

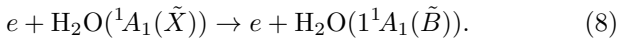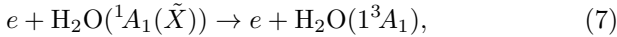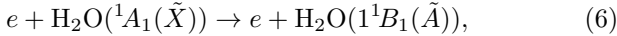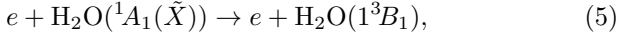$$e + \mathrm{H_2O}\,(j = 0) \rightarrow e + \mathrm{H_2O}\,(j = 1,\ 2,\ 3), \tag{2}$$
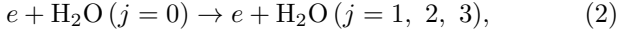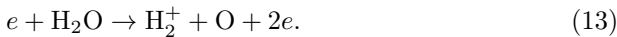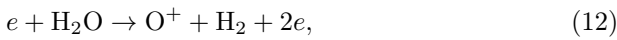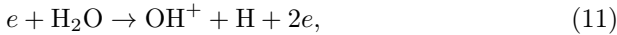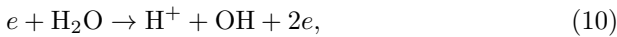
where j is the rotational quantum number;

3) vibrational excitations,

$$e + \mathrm{H_2O}(000) \rightarrow e + \mathrm{H_2O}(100),$$
$$e + \mathrm{H_2O}(000) \rightarrow e + \mathrm{H_2O}(001), \tag{3}$$
$$e + \mathrm{H_2O}(000) \rightarrow e + \mathrm{H_2O}(010). \tag{4}$$

4) electron excitation of the four lowest electron states of a water molecule,

$$e + \mathrm{H_2O}(^1A_1(\tilde{X})) \rightarrow e + \mathrm{H_2O}(1^3B_1), \tag{5}$$
$$e + \mathrm{H_2O}(^1A_1(\tilde{X})) \rightarrow e + \mathrm{H_2O}(1^1B_1(\tilde{A})), \tag{6}$$
$$e + \mathrm{H_2O}(^1A_1(\tilde{X})) \rightarrow e + \mathrm{H_2O}(1^3A_1), \tag{7}$$
$$e + \mathrm{H_2O}(^1A_1(\tilde{X})) \rightarrow e + \mathrm{H_2O}(1^1A_1(\tilde{B})). \tag{8}$$

5) ionization with generation of positive ions $\mathrm{H_2O^+}, \mathrm{H^+}, \mathrm{OH^+}, \mathrm{O^+},$ and $\mathrm{H_2^+}$,

$$e + \mathrm{H_2O} \rightarrow \mathrm{H_2O^+} + 2e, \tag{9}$$
$$e + \mathrm{H_2O} \rightarrow \mathrm{H^+} + \mathrm{OH} + 2e, \tag{10}$$
$$e + \mathrm{H_2O} \rightarrow \mathrm{OH^+} + \mathrm{H} + 2e, \tag{11}$$
$$e + \mathrm{H_2O} \rightarrow \mathrm{O^+} + \mathrm{H_2} + 2e, \tag{12}$$
$$e + \mathrm{H_2O} \rightarrow \mathrm{H_2^+} + \mathrm{O} + 2e. \tag{13}$$

6) dissociative sticking with generation of negative ions $\mathrm{OH^-}$, $\mathrm{H^-}$, and $\mathrm{O^-}$,

$$e + \mathrm{H_2O} \rightarrow \mathrm{O^-} + \mathrm{H_2}, \tag{14}$$

$$e + \mathrm{H_2O} \rightarrow \mathrm{H^-} + \mathrm{OH}, \tag{15}$$
$$e + \mathrm{H_2O} \rightarrow \mathrm{OH^-} + \mathrm{H}. \tag{16}$$

7) dissociation by channels,

$$e + \mathrm{H_2O} \rightarrow \mathrm{O}(^3P) + \mathrm{H_2}(X) + e, \tag{17}$$
$$e + \mathrm{H_2O} \rightarrow \mathrm{OH}(X) + \mathrm{H}(n = 1) + e. \tag{18}$$
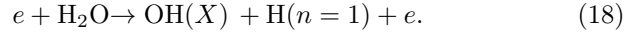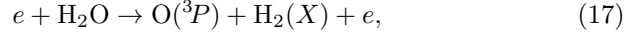
8) dissociative excitation by channels,

$$e + \mathrm{H_2O} \begin{cases} \rightarrow \mathrm{OH}^*(A) + \mathrm{H}(n = 1) + e, \\ \rightarrow \mathrm{O}^*(^1S) + \mathrm{H_2}(X) + e, \\ \rightarrow \mathrm{O}^*(3s^3S^0) + \mathrm{H_2}(X) + e, \\ \rightarrow \mathrm{OH}(X) + \mathrm{H}^*\ (n = 2, 3, 4) + e. \end{cases} \tag{19}$$
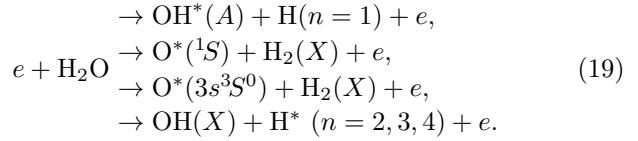
For processes (1)–(4) and (9)–(22), we used the dependences of cross-sections on the electron energy recommended in work [10]. For the electron excitation (5)–(8), we used the cross-sections theoretically calculated in work [11]. We did not manage to find the cross-sections for dissociation by the channel $e + \mathrm{H_2O} \rightarrow \mathrm{OH}(X) + \mathrm{H}(n = 1) + e$ in the literature; therefore, we used the same cross-sections as for the process $e + \mathrm{H_2O} \rightarrow \mathrm{O}(^3P) + \mathrm{H_2}(X) + e$.

By using the program Bolsig+, we calculated the EEDF in the stationary local approximation by solving the kinetic Boltzmann equation in the two-term approximation [9]. After having solved the kinetic Boltzmann equation, the average energy of electrons is calculated according to the relation $\bar{\varepsilon} = \int_0^\infty \varepsilon^{3/2} F_0\, d\varepsilon$, where $\varepsilon = (u/\gamma)^{1/2}$ is the kinetic energy of an electron; $\gamma = (2e/m)^{1/2}$; e, m, and u are the charge, mass, and velocity of an electron, respectively; and F_0 is the isotropic part of EEDF, which is normalized by the relation $\int_0^\infty \varepsilon^{1/2} F_0 d\varepsilon = 1$.

The normalized transport coefficients for electrons are calculated by the formulas [9] $\mu N = -\frac{\gamma}{3} \int_0^\infty \frac{\varepsilon}{\sigma_m} \times \frac{\partial F_0}{\partial \varepsilon} d\varepsilon$ and $DN = -\frac{\gamma}{3} \int_0^\infty \frac{\varepsilon}{\sigma_m} F_0 d\varepsilon$.

The drift velocity of electrons, u, is determined by the expression $u = \mu E = \mu N \times \frac{E}{N}$. Here, μ and D are the mobility and the diffusion coefficient of electrons, respectively; N is the concentration of atoms, $\sigma_m = \sum_j x_j \sigma_j$, σ_j is the effective cross-section of momentum transfer at elastic collisions of electrons with atoms and molecules; and x_j is the molar fraction of the j-th component in a gas mixture.

The rate constants of elementary processes were calculated by the formula $k_k = \gamma \int_0^\infty \varepsilon \sigma_k F_0 d\varepsilon$, where σ_k is the effective cross-section of inelastic collision.
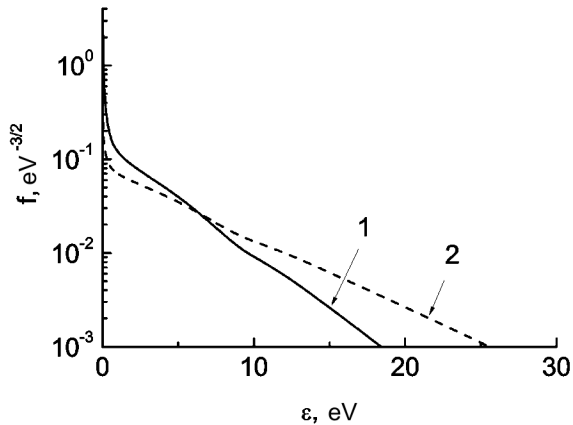
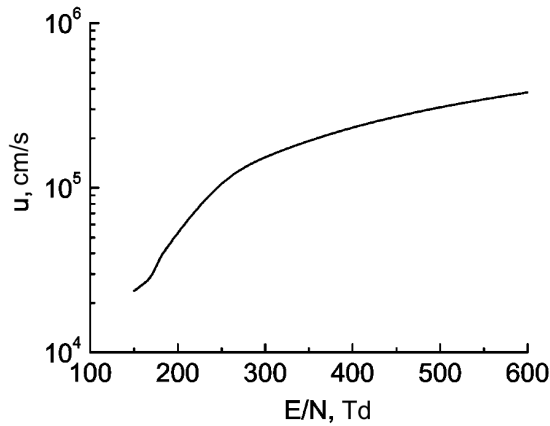**Fig. 1.** EEDFs in the water vapor discharge at the reduced electric field $E/N = 300$ (*1*) and 500 Td (*2*)

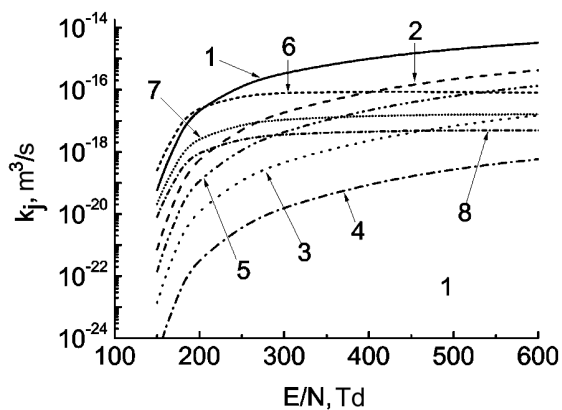**Fig. 2.** Drift velocity of electrons in the water vapor discharge as a function of the reduced electric field E/N

Fig. 3. Rate constants for dissociation, ionization, and dissociative sticking of electrons for H_2O^+ (*1*), OH^+ (*2*), H_2^+ (*3*), O^+ (*4*), H^+ (*5*), H^- (*6*), O^- (*7*), and OH^- (*8*) ions

118

The electron energy losses $\eta_k = \frac{\delta\varepsilon_k}{\sum_k \delta\varepsilon_k}$ were calculated by the formula $\eta_k = \frac{k_k n x_j N \Delta\varepsilon_k}{\sum_{k,j} k_k n x_{j=} N \Delta\varepsilon_k}$, where $\delta\varepsilon_k$ is the electron energy losses in the k-th process, $\sum_k \delta\varepsilon_k$ is the total electron energy losses, $\Delta\varepsilon_k$ is the threshold energy for the inelastic process, $\Delta\varepsilon_k = \frac{2m}{M_j}\bar{\varepsilon}$ for elastic collisions, and M_j is the mass of the j-th component in the gas mixture.

3. Calculation Results and Their Discussion

In Fig. 1, the EEDFs in the water vapor discharge calculated for the reduced electric fields $E/N = 300$ and 500 Td are depicted. One can see that, at electron energies lower than 0.5 eV, the EEDF is close to the Maxwellian one. However, for larger electron energies, the deviation of EEDF from the Maxwellian distribution grows. With increase in the ratio E/N, the slope of EEDF decreases, which testifies to the growth of the electron temperature. At electron energies lower than 0.5 eV, the slope of EEDF is very large, which means that a very low temperature and a very low average energy are typical of this range of electron energies.

The dependence of the electron drift velocity u on the reduced electric field E/N is plotted in Fig. 2. The growth of the electric field results in the increase of both the drift velocity and the average energy of electrons. The growth of the drift velocity with E/N is explained by the increase of the directed velocities of electrons, which they have on the mean free path. When being scattered by water molecules, electrons lose their directed velocity, and the energy associated with the directed motion of electrons transforms into the energy of their chaotic thermal motion. Therefore, the average energy of electrons also increases with E/N.

At $E/N < 150$ Td, the average energy of electrons does not exceed 0.2 eV. Such energies are rather low, being not sufficient to provide a required degree of plasma ionization. As a result, the maintenance of a discharge in water vapor is impossible at such E/N-values. In a low-temperature gas-discharge plasma, the typical average energies of electrons amount to 1–3 eV.

In Fig. 3, the dependences of the dissociation, ionization, and dissociative sticking rate constants on the reduced field E/N are exhibited. The dissociation rate for water molecules has the largest value for all E/N-values, which is connected with a large

dissociation cross-section (its maximum value equals 2.1×10^{-16} cm^2) and a low threshold energy (5.1 eV).

In the given model of barrier discharge in water vapor, the emergence of five positive and three negative ions is taken into account. The positive ions are generated in processes (9)–(13) of water molecule ionization [10]. At every E/N-value, the ionization rate for a water molecule with the formation of a water ion is substantially higher than the ionization rates for processes (10)–(13). The latter are accompanied by the water molecule dissociation, so that higher threshold energies and smaller cross-sections are inherent to them. The ion formation rate constant decreases along the sequence H_2O^+, OH^+, H^+, O^+, and H_2^+. This means that the main primary positive ion that emerges in a water vapor barrier discharge plasma is ion H_2O^+. As the quantity E/N grows, the rate constants of all ionization processes increase. The differences between the rate constants diminish, as the reduced electric field increases.

Negative ions are generated in the dissociative sticking reactions (14)–(16). The rate constants for negative ion formation reach their maxima in the E/N-range from 400 to 600 Td; afterward, they slowly decrease.

In Fig. 4, the dependences of the rate constants for the generation of negative and positive ions normalized to the rate constant of ion H_2O^+ formation on E/N are shown. The figure illustrates the dynamics of formation and disappearance of ions in relation to the applied field magnitude and the water vapor concentration. At $E/N < 170$ Td, the rates of positive and negative ion generation are close to each other, which should probably result in a low concentration of electrons in plasma and, as a consequence, a low plasma conductivity. At $E/N > 170$ Td, the discrepancy between the integrated rate constants of ionization and dissociative sticking starts to quickly increase. Plasma becomes electropositive, and its conductivity quickly grows, because the rate of electron generation exceeds the rate of negative ion generation very much.

The dependences of the relative weights of electron energy losses on the reduced field E/N at electron collisions of various types with water molecules are depicted in Fig. 5. The figure exhibits the reduced-field dependences of total energy losses at elastic collisions (Eq. (1)), energy losses for the excitation of rotational (Eq. (2) and vibrational
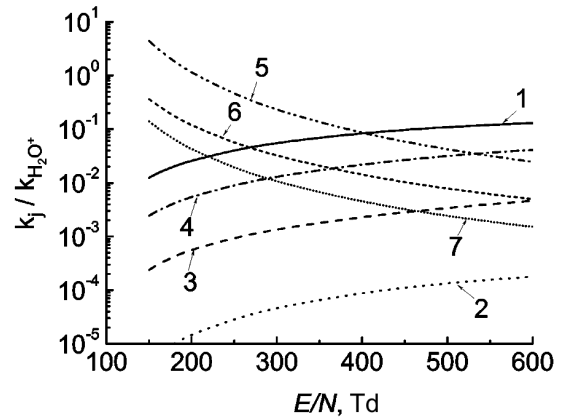

Fig. 4. Rate constants for ion generation in the water vapor discharge normalized by the rate constant for ion H_2O^+ generation as functions of E/N for various positive and negative ions: OH^+ (*1*), H_2^+ (*2*), O^+ (*3*), H^+ (*4*), H^- (*5*), O^- (*6*), and OH^- (*7*)
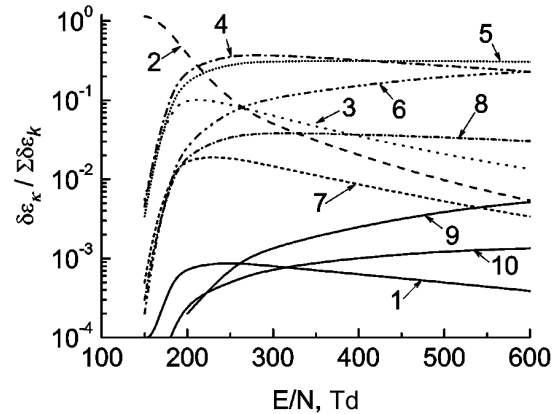

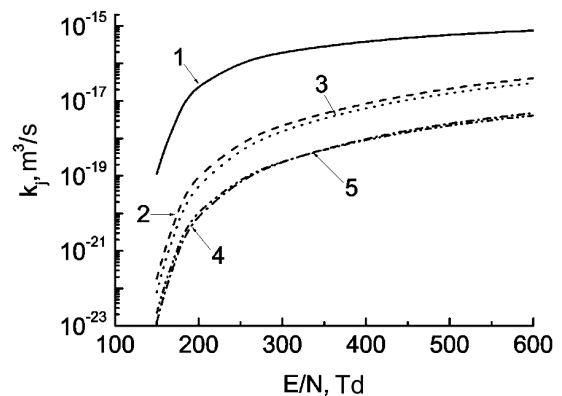**Fig. 5.** Dependences of the energy losses of electrons at their collisions with water molecules on E/N

Fig. 6. Rate constants for the dissociative excitation of OH* radicals and H* and O* atoms: $OH^*(A^2\Sigma^+)$ (*1*), $H^*(n=2)$ (*2*), $H^*(n=3)$ (*3*), $H^*(n=4)$ (*4*), and $O^*(3s^3S_0)$ (*5*)

(Eq. (3)) levels of water molecules in the ground state, energy losses for the excitation of electron levels (Eq. (4)), integrated energy losses in dissociation (Eq. (5)), ionization (Eq. (6)), and dissociative sticking (Eq. (7)) processes, and energy losses for the dissociative excitation of OH* radicals (Eq. (8)), hydrogen H* (Eq. (9)) and oxygen O* (Eq. (10)) atoms.

From Fig. 5, one can see that the electron energy losses for the excitation of rotational states of water molecules prevail at $E/N < 170$ Td. At low electron energies, this process runs very efficiently, and a good deal of energy obtained by electrons from the electric field is spent on the excitation of rotational levels. With the increase of E/N, the electron energy losses for the excitation of rotational states of water molecules decrease so that the main channels of electron energy losses within the field interval from approximately 200 to 500 Td are the excitation of electron states in water molecules and their dissociation. For instance, at $E/N = 400$ Td, approximately 36% of the electron energy is spent on the electron excitation of water molecules, the same amount on the dissociation, 16% on the ionization, 4% on the dissociative excitation of OH* radicals, 4% on the excitation of vibrations in H_2O molecules, 2% on the excitation of rotational levels in them, 1% on the dissociative sticking of electrons, and less than one percent on the dissociative excitation of hydrogen H* and oxygen O* atoms and the elastic scattering of electrons.

At $E/N \approx 600$ Td, the electron energy losses for the ionization become comparable with those for the excitation of electron states.

The electron energy losses in other processes, such as the excitation of rotational and vibrational states, dissociative sticking, dissociative excitation, and elastic collisions do not exceed 10% at $E/N > 170$ Td and diminish with the growth of E/N.

In Fig. 6, the rate constants for the dissociative excitation of OH* radicals, as well as H* and O* atoms, are shown. One can see that the rate constant for the dissociative excitation of OH* radicals exceeds the corresponding parameter for hydrogen H* ($n = 2$) and H* ($n = 3$) atoms by more than one order of magnitude, and by almost two orders of magnitude for hydrogen H* ($n = 4$) and oxygen O* atoms. When the reduced electric field E/N

grows, the rate constants for the dissociative excitation of hydrogen H* ($n = 2$), H* ($n = 3$), and H* ($n = 4$) states increase faster in comparison with that of OH* radical. This means that the intensity of hydrogen lines belonging to the Balmer series will increase more strongly with the growth of E/N in comparison with the intensity of bands corresponding to hydroxyl OH*.

The results obtained in this work can be used for modeling the plasma kinetics in the water vapor barrier discharge.

4. Conclusions

The results of our calculations concerning the rate constants for the processes of electron collisions with water molecules, which were obtained by solving the kinetic Boltzmann equation, show that excited OH* ($A^2\Sigma^+$) radicals in the water vapor discharge appear in the course of the dissociative excitation process, when collisions of electrons with water molecules take place. The generation rate of OH*($A^2\Sigma^+$) radicals in the water vapor discharge is substantially higher than that of emitting states of hydrogen and oxygen atoms. According to our estimations, the rate constant for the dissociative excitation of OH*(A) radical increases with the reduced electric field, and the relative electron energy losses for the excitation of OH*($A\,^2\Sigma^+$) radical reach a maximum at about 350 Td. The optimum values of reduced electric field for the excitation of OH*($A^2\Sigma^+ \to X^2\Pi$) bands in the water vapor discharge amount to 300–400 Td, because the growth of the rate constant for the dissociative excitation of hydroxyl OH*($A^2\Sigma^+$) molecules slows down at $E/N > 400$ Td, whereas the electron energy losses for the excitation of OH*($A^2\Sigma^+$) attain their maximum.

1. M.I. Lomaev, V.S. Skakun, E.A. Sosnin, V.F. Tarasenko, D.V. Shitts, and M.V. Erofeev, Usp. Fiz. Nauk **173**, 201 (2003).
2. U. Gross, A. Ubelis, and P. Spietz, J. Phys. D **33**, 1588 (2000).

3. A.Ya. Vul', S.V. Kidalov, V.M. Milenin, N.A. Timofeev, and M.A. Khodorkovskii, Pis'ma Zh. Tekhn. Fiz. **25**, 10 (1999).

4. A.K. Shuaibov, I.V. Shevera, and A.A. General, Zh. Prikl. Spektrosk. **73**, 831 (2006).

5. F. Morozov, R. Kruchen, T. Ottenhal, and A. Ulrich, Appl. Phys. Lett. **86**, 011502 (2005).

6. A.K. Shuaibov, A.A. General, V.A. Kel'man, and I.V. Shevera, Pis'ma Zh. Tekhn. Fiz. **34**, 6 (2008).

7. E.A. Sosnin, M.V. Erofeev, S.M. Avdeev, and A.N. Panchenko, Kvant. Elektron. **36**, 981 (2006).

8. A.A. General, Yu.V. Zhmenyak, V.A. Kel'man, and Yu.O. Shpenik, Nauk. Visnyk Uzhgorod Univ. Ser. Fiz. **29**, 249 (2011).

9. G.J.M. Hagelaar and L.C. Pitchford, Plasma Sources Sci. Technol. **14**, 722 (2005).

10. Y. Itikawa and N. Mason, J. Phys. Chem. Ref. Data **34**, 1 (2005).

11. J.D. Gorfinkiel, L.A. Morgan, and J. Tennyson, J. Phys. B **35**, 543 (2002).

А.А. Генерал, Ю.О. Шпеник

МОДЕЛЮВАННЯ ГАЗОВОГО РОЗРЯДУ
В ПАРАХ ВОДИ

Р е з ю м е

Представлено результати дослідження газорозрядної плазми парів води. Швидкість утворення збуджених радикалів OH* ($A^2\Sigma^+$) в розряді в парах води значно вище швидкостей утворення випромінювальних станів атомів водню і кисню. Згідно з оцінками оптимальні для збудження смуг радикала OH* значення E/N (тут E – напруженість електричного поля, N – концентрація частинок газу) становлять 300–400 Тд.